NPS62-90-011

NAVAL POSTGRADUATE SCHOOL

Monterey, California

COMPUTER MODEL OF A HIGH-RESOLUTION IMAGING SONAR

Rajendar Bahl
and
John P. Powers

June 1990

Prepared for:
Naval Postgraduate School
Monterey, CA 93943

NAVAL POSTGRADUATE SCHOOL
Monterey, CA

Rear Admiral R.W. West, Jr.
Superintendent

Dr. Harrison Shull
Provost

This report was prepared in conjunction with a National Research Council Senior Research Associateship awarded to Rajendar Bahl.

This report was prepared by:

REPORT DOCUMENTATION PAGE

Form Approved
OMB No. 0704-0188

1a REPORT SECURITY CLASSIFICATION UNCLASSIFIED	1b RESTRICTIVE MARKINGS
2a SECURITY CLASSIFICATION AUTHORITY	3 DISTRIBUTION/AVAILABILITY OF REPORT
2b DECLASSIFICATION/DOWNGRADING SCHEDULE	
4 PERFORMING ORGANIZATION REPORT NUMBER(S) NPS62-90-011	5 MONITORING ORGANIZATION REPORT NUMBER(S)
6a NAME OF PERFORMING ORGANIZATION Naval Postgraduate School 6b OFFICE SYMBOL (*If applicable*)	7a NAME OF MONITORING ORGANIZATION National Research Council
6c ADDRESS (*City, State, and ZIP Code*) Monterey CA 93943	7b ADDRESS (*City, State, and ZIP Code*) Attn: Associateship Programs 2101 Constitution Ave. Washington DC 20418
8a NAME OF FUNDING/SPONSORING ORGANIZATION National Research Council 8b OFFICE SYMBOL (*If applicable*)	9 PROCUREMENT INSTRUMENT IDENTIFICATION NUMBER
8c ADDRESS (*City, State, and ZIP Code*) Attn: Associateship Programs 2101 Constitution Ave. Washington DC 20418	10 SOURCE OF FUNDING NUMBERS PROGRAM ELEMENT NO / PROJECT NO / TASK NO / WORK UNIT ACCESSION NO

11 TITLE (*Include Security Classification*)
COMPUTER MODEL OF A HIGH-RESOLUTION IMAGING SONAR

12 PERSONAL AUTHOR(S)
Rajendar Bahl and John Powers

13a TYPE OF REPORT	13b TIME COVERED	14 DATE OF REPORT (*Year, Month, Day*)	15 PAGE COUNT
Technical	FROM Aug 89 TO Jun 90	1990, July 1	

16 SUPPLEMENTARY NOTATION

17 COSATI CODES			18 SUBJECT TERMS (*Continue on reverse if necessary and identify by block number*)
FIELD	GROUP	SUB-GROUP	Acoustic imaging, Sonar, Computer simulation, target model, Backscatter, 3-D reconstruction, Acoustic shadow, Silhouette, Segmentation

19 ABSTRACT (*Continue on reverse if necessary and identify by block number*)

A computer model of a high-resolution sector-scanning sonar used for imaging objects against the sea bottom is presented. The model accounts for the sonar parameters, bottom backscatter, reflections from the target's visible surface, and the target's acoustic shadow. A variety of imaging scenarios can be simulated including the type of target, the target's orientation relative to the sonar and the bottom, and the backscatter statistics. The acoustic images are presented in the conventional B-scan format. A new display format that is useful for visualizing the target's silhouette is also presented. Visual perspective images of the scene are presented to serve as a reference for subsequent image reconstruction work. Preliminary results for 3-d reconstruction of the confining volume of the visible target surface are also presented. The simulation model and the results of the 3-d reconstruction demonstrate the promise of the application of image processing techniques for classification of objects using acoustic images.

20 DISTRIBUTION/AVAILABILITY OF ABSTRACT	21 ABSTRACT SECURITY CLASSIFICATION
☒ UNCLASSIFIED/UNLIMITED ☐ SAME AS RPT ☐ DTIC USERS	Unclassified
22a NAME OF RESPONSIBLE INDIVIDUAL Professor John Powers	22b TELEPHONE (*Include Area Code*) (408) 646-2081 / 22c OFFICE SYMBOL

COMPUTER MODEL OF A HIGH–RESOLUTION IMAGING SONAR

Rajendar Bahl[1] and John P. Powers
Department of Electrical and Computer Engineering
Naval Postgraduate School
Monterey, CA 93943

June 14, 1990

[1]National Research Council Senior Research Associate on leave from Indian Institute of Technology, New Delhi 110016, India.

ABSTRACT

A computer model of a high-resolution sector-scanning sonar used for imaging objects against the sea-bottom is presented. The model accounts for the sonar parameters, bottom backscatter, reflections from the target's visible surface, and the target's acoustic shadow. A variety of imaging scenarios can be simulated including type of target, the target's orientation relative to the sonar and the bottom, and the backscatter statistics. The acoustic images are presented in the conventional B-scan format. A new display format that is useful for visualizing the target's silhouette is also presented. Visual perspective images of the scene are provided to serve as a reference for subsequent image reconstruction work. Preliminary results for 3-d reconstruction of the confining volume of the visible target surface are also presented. The simulation model and the results of the 3-d reconstruction demonstrate the promise of the application of image processing techniques for classification of objects using acoustic images.

Contents

List of Figures

Chapter 1

IMAGING SONARS AND THEIR SIMULATION

1.1 INTRODUCTION

High–resolution sonar is the generic name for high frequency sonars that are conventionally used for imaging applications in a variety of areas like sea–bottom profiling, mine–hunting, undersea–navigation, diver guidance, surveillance, etc. These sonars typically use frequencies in the range 100 kHz – 2 MHz depending on the application; the higher the sonar frequency, the better are the range and bearing resolution [1,2,3]. Even so, the image quality presently obtainable from these sonars for realistic acoustic apertures is far inferior to that of an optical sensor. However, the main advantage of using acoustic sensors is the potential for relatively longer ranges, more so in turbid waters. It is this range capability that makes sonar an indispensable sensor in hostile underwater imaging applications.

1.2 REVIEW

Historically, the first imaging sonar was the side–scan sonar or the side–look sonar [1]. This sonar is typically mounted on a tow–fish that is towed behind the mother–ship. The tow–fish has a horizontal linear array on either side for looking at a narrow bottom swath at right angles to the ship's track. As the ship moves (in a straight line or a well–defined track) the sonar obtains

the range profile of the sea bottom very much like a searchlight beam. It is obvious that the scanning speed (i.e., the ship speed) is limited by the time taken for the acoustic signal to traverse the two–way distance to the farthest point in a given swath. In spite of the slow speed of scan, the side–scan sonar is a standard for hydrographers for the generation of sea–bottom maps and profiles of interesting undersea features.

The next evolution in imaging sonars was the development of the sector–scanning sonar [2]. These sonars have the ability to scan an angular sector from a static location by means of electronic scanning of the acoustic beam (very much like a phased–array radar). The beam scanning technology has been continually updated from analog to the modern digital techniques. The sonar transmits a cw pulse in a horizontally wide beam of approximately 30° beamwidth that insonifies the sector of interest. This sector is rapidly scanned immediately thereafter by a narrow receiver beam of typically 1° beamwidth once every range cell (as defined by the pulsewidth). This is a very efficient method of obtaining images in near–real–time. These sonars have found wide use in underwater vehicles and submersibles.

The sonars discussed above produce images that represent the acoustic backscatter of various features on the sea bottom from the particular aspect of the sonar. The acoustic images are, therefore, 2–d intensity images of the 3–d scene and disregard the height of the reflecting features, the images being a modified plan view. Further attempts have been made to obtain orthographic images very much like the optical camera [3]. Some of these sonars use holographic techniques for image formation of 3–d objects in the near–field region of the planar apertures. The imaging process and the transducer hardware complexity of these sonars is very high which has precluded their widespread use as compared to side–scan and sector–scan sonars.

Apart from the above real–aperture imaging sonars there are other implementations that address the problems of resolution (both azimuthal and range) and blind range. Some notable implementations are the synthetic aperture sonar, the continuous–time frequency–modulation (CTFM) sonar, and the wideband monopulse sonar [4,5,6]. However, these techniques do not completely solve the inherent image quality problems of acoustic imaging and have their own domain of application.

1.3 MOTIVATION

This report is the outcome of an ongoing investigation relating to acoustic imaging and classification of objects on the sea bottom. In this work we are interested in obtaining images of 3–d objects lying on the sea bottom (which is considered to be flat in the region of the object). The imaging geometry for such an application is a sonar that is looking down towards the object from a stand–off location above and in front of the object (Fig. 1.1). The actual distance depends on the object size and the sonar parameters required to obtain the best resolution. Our attempt here is to obtain perspective images of 3–d objects by means of a simulated sector–scanning sonar using a linear array. It is obvious that a linear array having only azimuthal resolving power cannot, by itself, generate 3–d images unless some other information is available. In our study, we are hoping to utilize additional information. For example, the shadows and echo intensity could be useful for reconstructing the missing elevation information of the object.

In view of the above, it is apparent that a need exists to first simulate realistic acoustic images from a sector–scanning sonar including shadow effects. These acoustic images can be used as a test–bed for the design of algorithms for 3–d image generation and object classification. Previous simulation work in this area has considered objects to be flat regions (on the sea bottom) of appropriate reflectivity [7]. This assumption falls short of a realistic simulation study. In this report we outline the simulation model of an imaging sonar for a more authentic 3–d scenario and also show some preliminary results of 3–d imaging. It is hoped that the techniques developed in this process would be applicable to the acoustic images obtained by sector–scanning sonars in the real–world.

1.4 RELEVANCE OF THE SIMULATIONS

A computer simulation model of an imaging sonar for developing advanced imaging and classification algorithms has a number of applications. Measurements at–sea are known to be highly expensive in terms of time, money and a host of other support and resources. The sea is also a highly variable medium that makes controlled measurements a formidable challenge. In this context an exercise for simulating controlled measurements becomes a rela-

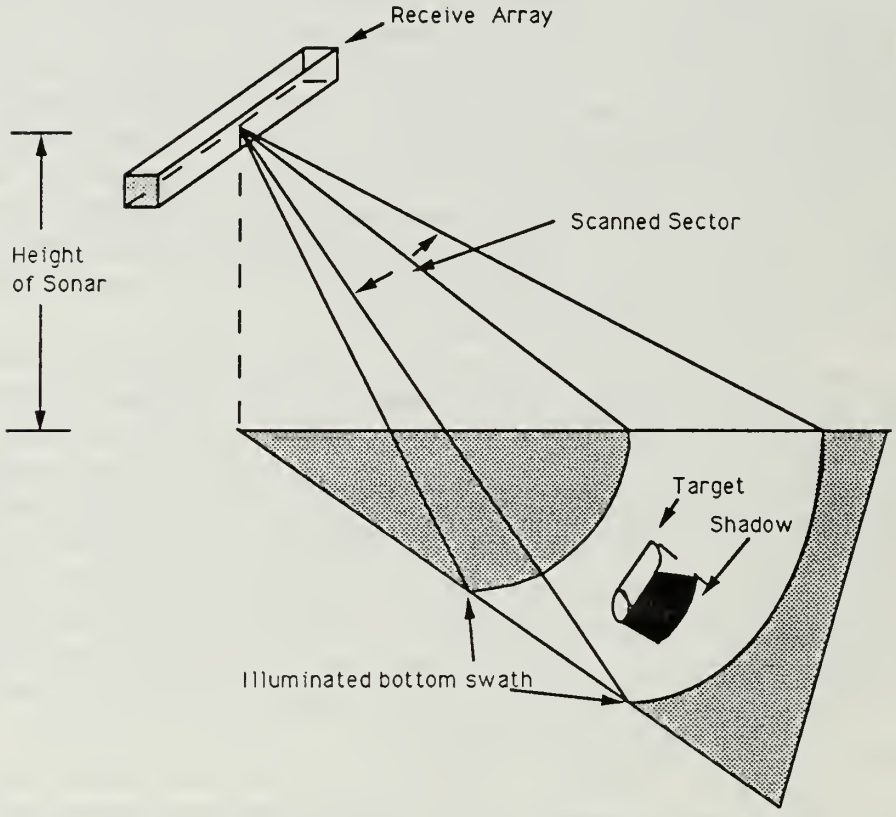

Figure 1.1: SECTOR-SCANNING IMAGING SONAR GEOMETRY

tively inexpensive alternative. Over the years a lot of data of a statistical nature pertaining to various aspects of propagation has been made available. While the applicability of this data in a particular situation is questionable, it can certainly be useful in a modeling exercise. In our case of imaging of 3–d objects we adopt statistical models for the bottom backscatter instead of generating actual backscatter from individual scatterers on the sea floor (and the reflecting layers below). However, we attempt a complete simulation of the target's scattering surface. The effect of such a methodology is to generate close to realistic acoustic images against a standardized backscattering sea floor.

Another benefit of a simulation model is its use as a tool for the design of the sonar itself. The various user–selectable parameters of the sonar, the target, the backscatter, and the imaging geometry can be used to optimize the sonar design in an interactive manner.

And finally, the sonar model can be used for training sonar operators in various imaging scenarios.

The following chapters present the step–wise evolution of the computer model. Chapter 2 introduces the strategy adopted for the entire simulation study which is then elaborated in the subsequent chapters. In chapter 3 we discuss the implementation of the target models, the imaging geometry, and the generation of visual perspective image of the scene that is to be imaged by the sonar. The computation of the target data required for echo formation by the sonar is also discussed. Chapter 4 presents the main acoustic imaging program wherein the sonar's parameters, backscatter characteristics, and the target data are used in the formation of B–scan images. These images demonstrate the targets' specular echoes and their shadows on the sea bottom. A new display that presents the silhouette of the target is also discussed. In chapter 5 we discuss our first attempts at 3–d reconstruction of the targets from their acoustic images. The results in the form of wire–frame images of the confining volume of a target's visible surface are presented. Chapter 6 concludes the report with some thoughts on possible enhancements of the computer model. A brief operating guide for running the software is presented in the Appendix to the report.

Chapter 2

COMPUTER MODELING STRATEGY

2.1 INTRODUCTION

The entire simulation model was implemented on an IBM PC–AT (or compatible) computer. It was written in Microsoft FORTRAN 4.01. The acoustic and perspective images generated by this software were displayed and recorded by using a PC–based image processing system "PCVISIONplus" from Imaging Technology, Inc. The hardcopy unit is Tektronix model HC01 Video Processor Unit. The computer model interacts with the user/operator for setting up various options and parameters for the imaging scenario. The following sections briefly discuss the methodology adopted in the simulation exercise.

2.2 THE SONAR MODEL

The sonar is modeled as a typical high–resolution sector–scanning sonar with the following programmable parameters:

- receiver beamwidth,
- range resolution, and
- wavelength.

Sonar (name/type)	Sector coverage (degrees)	Receiver beamwidth horizontal (degrees)	Receiver beamwidth vertical (degrees)	Scan rate (kHz)	Frequency (kHz)
NUTDI	30	1	—	8	500
Hydrosearch	60	0.5	8.5	7.5	180
Type 193	16	1	20	—	100
Bifocal	30	0.33	10	10, 30	305

Table 2.1: Parameters of some representative imaging sonars. (adapted from [2])

The transmitter is presumed to uniformly insonify a certain azimuth sector which is scanned by vertical fan beams of the receiver (Fig. 2.1). This model can be used to represent some practical and commercially available imaging sonars as represented in Table 2.1. The echo formation process is based on the coherent summation of the signals from the target's "visible" point scatterers/reflectors lying within a particular range–bearing resolution cell of the sonar [8]. The spreading and absorption losses for individual scatterers within the same resolution cell are considered to be equal. In addition, we have assumed that the sonar performs gain compensation for these losses over the entire range.

2.3 THE TARGET MODEL

The target is modeled as a densely packed (with respect to the wavelength) surface of point reflectors. In this study we have modeled spheres and cylinders which typify the features of many man–made objects. The targets can be arbitrarily oriented in the horizontal plane for presenting various attitudes towards the sonar. They can be positioned at any depth below the sonar or on the sea–bottom.

2.4 THE BACKSCATTER MODEL

The sea bottom is modeled as a flat surface that basically follows Lambert's law for acoustic backscatter at various grazing angles with an underlying

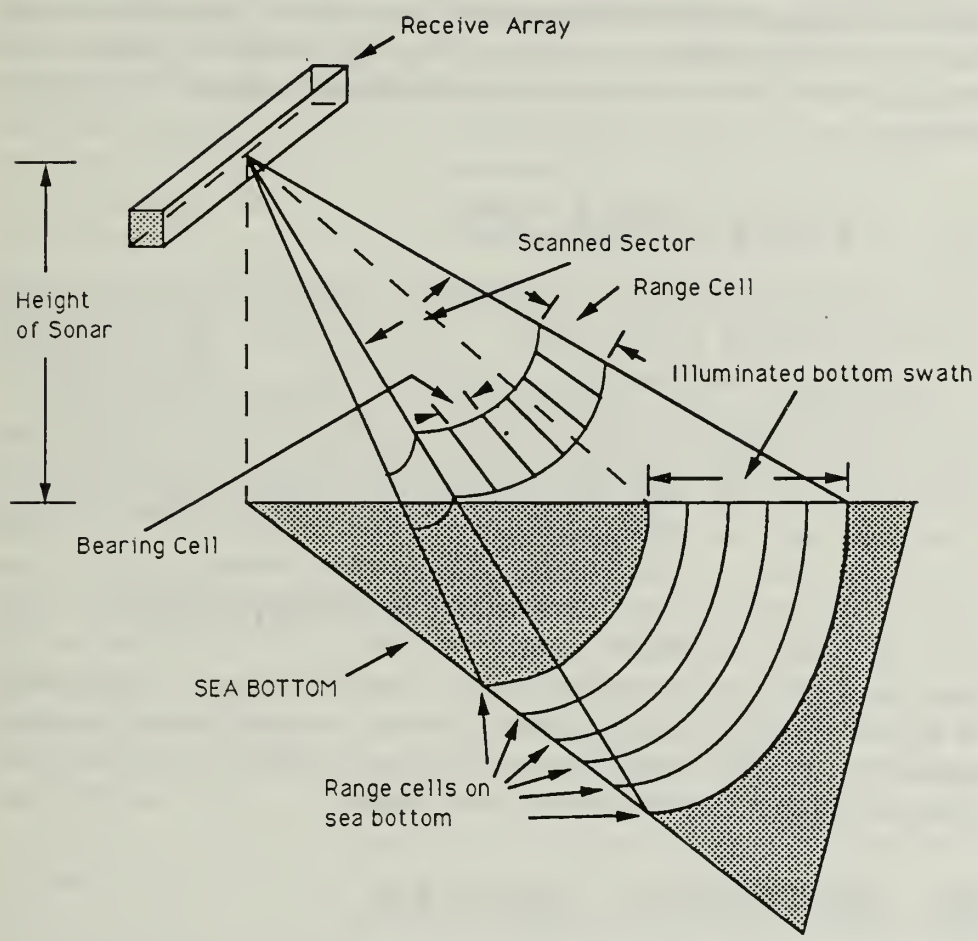

Figure 2.1: PRINCIPAL SONAR PARAMETERS

random variability [9,10,11]. The "exposed" area and the grazing angle of the bottom in every range–bearing cell is used for computing the total (deterministic) bottom backscatter. This is then (optionally) multiplied by a random number that defines the backscatter statistics. The exposed area in each range–bearing cell is computed by subtracting the area that falls in the acoustic shadow of the visible portion of the target from the total area. The random backscatter is statistically modeled as a number generated by a random process having either a uniform or Rayleigh probability density. This takes into account to some extent, the variability observed in the backscatter statistics.

2.5 VISUAL IMAGES

A perspective image as would be perceived by an optical camera at the sonar location is generated by the method of range shading. This image serves as a reference for the subsequent efforts for 3–d image generation using the acoustic imaging model. The visual image is generated by the principle of perspective projection using a pin–hole camera at the sonar location. The distance of the image plane from the pin–hole and the image size (250 x 250 pixels in our case) determine the size of the "visual pixels". Each pixel on the image plane, in turn, represents a certain solid–angle region in space which encompasses an increasing number of target voxels at larger distances from the camera. The nearest target voxel intercepted by the solid angle is imaged on that particular "visual pixel" to retain the opacity of the target. The xyz–coordinates of such imaged voxels are recorded for the purpose of acoustic imaging. The visual images are range–shaded and portrayed against a flat sea bottom for presentation to the viewer.

2.6 ACOUSTIC IMAGES

The object echo and the bottom backscatter are summed incoherently to get the resultant signal intensity in every range–bearing cell. The signal level is stored in the conventional "range vs. bearing" format referred to as "B–scan". Two images are generated: (i) target echo alone, and (ii) composite target echo and backscatter returns. The composite image is the

simulated acoustic image as simulated for a 3–d object against a sea bottom and demonstrates realistic features like acoustic shadow and specular returns.

2.7 SILHOUETTE IMAGE

A modified B–scan display format has been proposed in this work that serves as an aid for object classification. The knowledge of the height of the imaging sonar above the sea bottom can be used to warp the range scale to provide a perspective image of the flat sea bottom as viewed from the sonar. The resultant image is very effective in displaying the shadow of the object in the form of its true silhouette. In the situation that the object and shadow do not overlap in range, the silhouette shows the entire object's visible outline. For objects in contact with the sea bottom, the silhouette represents the object's upper outline. In either event the silhouette is a useful potential classifier of the object shape, more so because of the distracting speckled echoes within the object image.

The preceding sections have described the approach followed for the development of the conventional acoustic imaging program. The succeeding sections present image processing techniques that have been applied to the acoustic images generated by the above program.

2.8 SEGMENTATION

The composite acoustic B–scan image represents echoes from three distinct regions: the target, the sea bottom, and the shadow. The first thing to do as a step towards 3–d image reconstruction and classification is to automatically identify these regions. A program has been written that adaptively sets two thresholds at every range line. These thresholds are used as reference values to label each acoustic pixel as one of the three regions: an object point, a shadow point, or a sea–floor point. We have, at the present time, developed the segmentation algorithm for the simplified case of constant Lambertian backscatter so as not to detract from the immediate task of 3–d imaging and classification. The segmentation of speckled images is in itself a challenging problem and is the subject of other independent studies as well (see, for example, Ref. [12]).

The results of the segmentation serve as the first input towards 3–d reconstruction.

2.9 RAW 3–D IMAGES

The last topic discussed in this report is the generation of raw 3–d images from the segmentation data. These results are for the case when the target echo and its shadow do not overlap in range for a given bearing. The extent of the shadow at each bearing represents the vertical angular extent of the object in that bearing. The range and vertical extents of the object in all bearings are used to postulate that the visible portion of the object is confined within a particular volume. In the absence of other clues we cannot define the exact surface curve within the above volume.

The confining volume has been captured as a perspective image of a wire–frame model that can be viewed from various vantage locations including the actual sonar location. This procedure provides the user/operator with a feeling of depth of the confining volume of the object's visible surface.

We have presented above the broad outline of the computer model that has been implemented. In the following chapters we discuss the detailed implementation of the model and the results that have been obtained. We first start by discussing in the next chapter the imaging scenario, the target models, and the generation of visual images and target data required for computing the target's contribution to the acoustic image.

Chapter 3

THE IMAGING SCENARIO

3.1 INTRODUCTION

We have in this report considered the imaging of two types of targets, spheres and cylinders. The size of these objects and their orientation relative to the sonar and the sea bottom can be specified to formulate the imaging scenario. The targets are modeled as solid surfaces whose 3–d coordinates are computed and stored in disk files. The coordinates of the target voxels are stored in integer units. All other linear dimensions, for example, height of the sonar above the sea bottom, wavelength and range resolution of the sonar, etc. are referenced to the same units. The surface coordinates are used to generate the visual perspective images of the targets against the sea floor. Those voxels that get visually imaged are then stored for subsequent computation of the acoustic image of the target.

The basic building block is the "circle" with a radius of 100 units (say, centimeters). The coordinates around the circumference of this circle are computed and stored in a sequential formatted file called "CIRCLE". The points are computed at 1,000 equally–spaced locations around the circumference. (The run–file for this program is "CIRCLE.EXE".)

3.2 THE SPHERE MODEL

The sphere is constructed by stacking circles of appropriate radius one behind the other. In our model we construct the sphere of user–selected radius

($\leq$ 100 units) by stacking circles that represent transverse slices (along a principal diameter) taken every 1° inclination with the diameter. The coordinates of the representative circle are suitably scaled for the circular slices. The scaled coordinates are truncated to integer units and stored only if they are different from the previous point's coordinates. The entire 3–d coordinates of the sphere are stored in a sequential formatted file "SPHERE3". (The run–file for this program is "SPHERE3.EXE".)

3.3 THE CYLINDER MODEL

The cylinder's curved surface coordinates are computed by stacking circles of radius as selected for the cylinder at every 1 unit along the axis. The front and back faces of the cylinder are constructed by superimposing circles of radii increasing from 0 to the cylinder's radius in steps of 1 unit. The radius and length of the cylinder are selectable ($\leq$ 100 units). Once again, only those (quantized) coordinates around each circle are stored that are distinct from the previous point's coordinates. (This helps in reducing the memory storage requirements.) The cylinder's 3–d coordinates are stored in a sequential formatted file "CYL". (The run–file for this program is "CYL.EXE".)

3.4 PERSPECTIVE VISUAL IMAGES

The next step is to set up the imaging scenario based around one of the above target models. A program has been written that does the following:

- defines the world 3–d coordinate system with the sonar location as the origin,
- defines target location and orientation,
- defines sea–bottom location below the sonar,
- constructs a range–shaded perspective image of the opaque target and the flat sea–bottom as seen from the sonar location, and then
- generates a file that records target voxels that are visible in the perspective image.

The program accepts the 3-d coordinates of the selected target and first converts the coordinates to the world coordinates by taking into account the orientation of the target relative to the sonar (Fig. 3.1). Those target voxels that are below the sea-bottom are not considered. The target voxels and the sea-bottom are then perspectively imaged onto a vertical image plane that has the following parameters (Fig. 3.2):

- distance of the image plane from the sonar,
- image size of 250 x 250 pixels, and
- intensity recorded as an 8-bit binary number.

The perspective image is formed using the following formulas:

$$Y_i = \text{INT}\left(\frac{Y_t}{X_t} * F_i\right) + 125 \tag{3.1}$$

$$Z_i = \text{INT}\left(\frac{Z_t}{X_t} * F_i\right) + 125 \tag{3.2}$$

$$I_i = 127 - \text{INT}\left(\frac{R_t}{5}\right) \tag{3.3}$$

where

- Y_i is the y-coordinate on image plane,
- Z_i is the z-coordinate on image plane,
- F_i is the distance of the image plane from the origin,
- I_i is the image pixel intensity,
- X_t, Y_t, Z_t are the xyz-world coordinates of the target voxel, and
- $R_t = \sqrt{X_t^2 + Y_t^2 + Z_t^2}$ is the target voxel range.

The added constant of 125 in equations 3.1 and 3.2 ensures that the camera axis is imaged in the center of the image plane. Equation 3.3 allows the maximum image intensity to be 127 and the minimum as 0 at the range of 635 units. Care has to be taken while formulating the imaging scenario

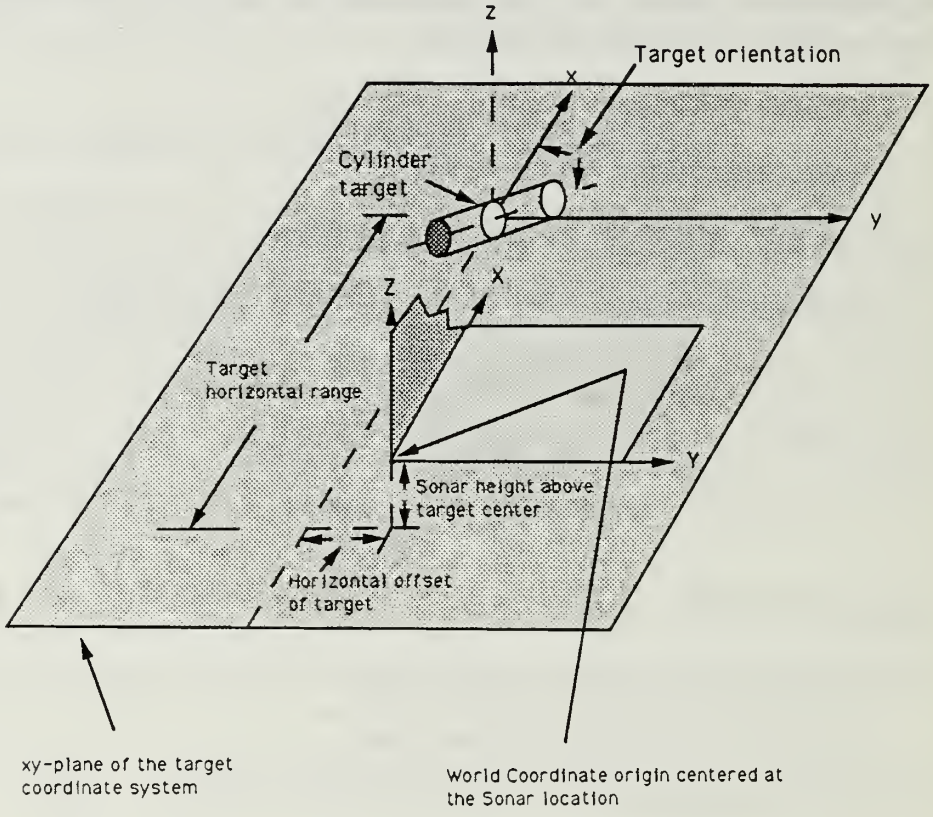

Figure 3.1: TARGET AND WORLD COORDINATE SYSTEMS

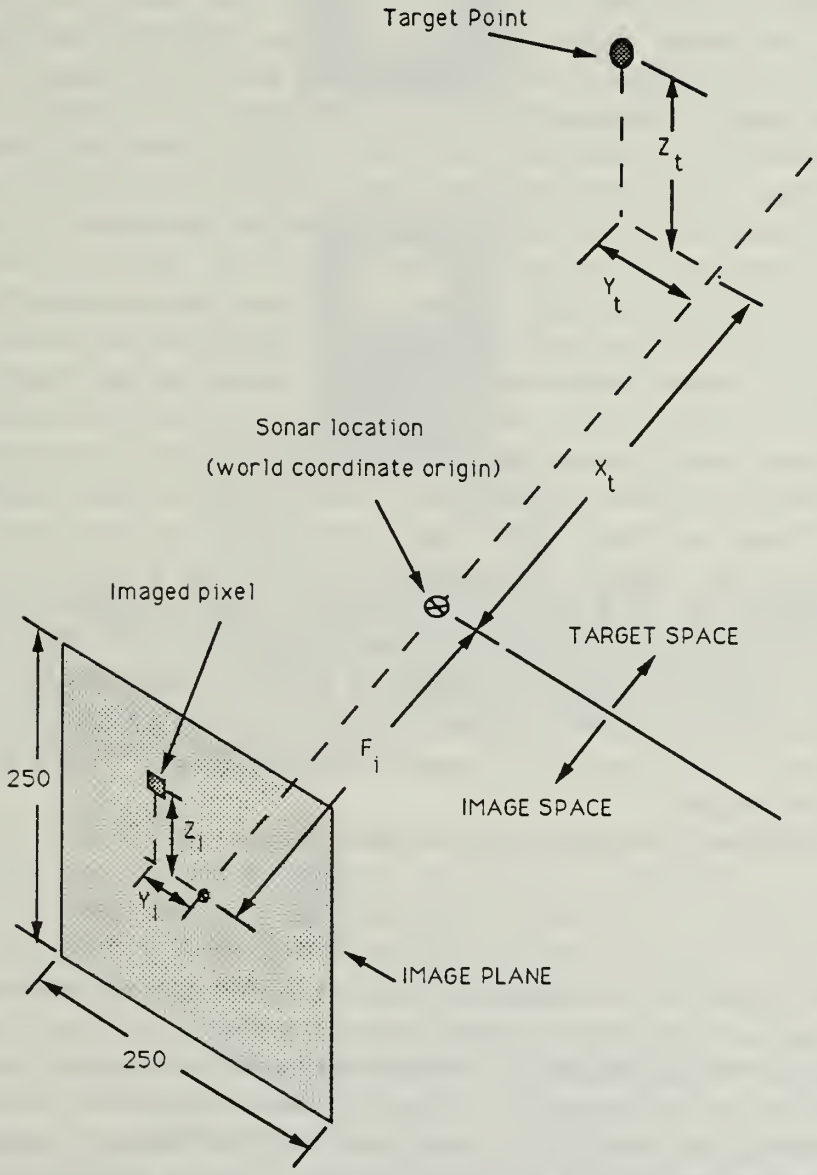

Figure 3.2: VISUAL PERSPECTIVE IMAGE GEOMETRY

that the maximum range of the target's visible extent does not exceed 635 units to prevent underflow in Eq. 3.3.

A pixel on the image plane represents a solid–angle region in space as implied by the equations 3.1 and 3.2. Thus, the actual surface area represented on the object by a particular pixel increases with the distance of the imaged object from the camera. (This, in fact, explains the perspective effect that distant objects appear smaller than when they are closer to the camera.) It is apparent that F_i governs the size of the image; the larger it is, the larger is the image and, hence, the better is the imaging resolution. It is, therefore, possible that more than one target voxel gets imaged at the same pixel. This would typically happen for the more distant target voxels. In such situations the program records the coordinates of the nearest voxel. This also automatically ensures that voxels "behind" others, (e.g., as at the far side of the target) do not get imaged, thus ensuring the target's opacity. On the other hand there is also the danger of over–resolution of the (granular) surface point–coordinates of the targets at near ranges. In such situations the perspective imaging would indicate a perforated hollow object and hence image the normally hidden far–side voxels of the target through the near–end surface "perforations". This anomaly is easily noticed in the visual image as "holes" in the image which are in fact low intensity points of the far–end surface. This potential problem can be fixed by the choice of a smaller F_i. As a first rule of thumb, F_i may be chosen to be at most half the horizontal distance of the nearest object point. This would force adjacent target voxels to be imaged on the same pixel thereby eliminating the possibility of "hole" formation. (There is another constraint on the lower limit of F_i arising out of the acoustic imaging aspect. This is discussed in the next chapter.)

The above constraint on F_i can be formulated as:

$$F_i < \frac{X_t(\min)}{2}, \tag{3.4}$$

where $X_t(\min)$ is the horizontal distance of the nearest target voxel.

The final perspective image in 250 x 250 format is recorded in a sequential binary file "PERSVIS3.IMG" in which the x–axis is represented as a point in the center of the image plane. This file is stored in a format that is suitable for viewing and hardcopying using the "PCVISIONplus" system. Sample images for a sphere and a cylinder suspended above the bottom are shown

(a)

(b)

Figure 3.3: SAMPLE VISUAL PERSPECTIVE IMAGES OF SUSPENDED TARGETS. a) Sphere with radius of 100 cm, b) Cylinder with 100 cm radius and 100 cm length. (Height of target center above bottom = 150 cm, horizontal distance from sonar = 450 cm, sonar height = 350 cm, distance of image plane behind sonar=100 cm.)

in Figure 3.3. Both objects have their centers 150 cm above the sea–bottom. The cylinder has its axis horizontal and presents a broadside view to the camera. The range shading provided in these images gives a feeling of depth in the image. Since the sea–bottom is quite far off, its intensity is close to zero and is therefore not perceptible against the background for these suspended objects.

Figure 3.4 shows sample images of these objects half–submerged in the sea bottom. The object centers lie exactly on the sea bottom and so the lower halves of the objects are submerged. The cylinder is horizontal and oriented at 45° with respect to the x–axis of the target coordinate system. The center is offset by 100 cm along the y–axis (see Fig. 3.1). The sea bottom

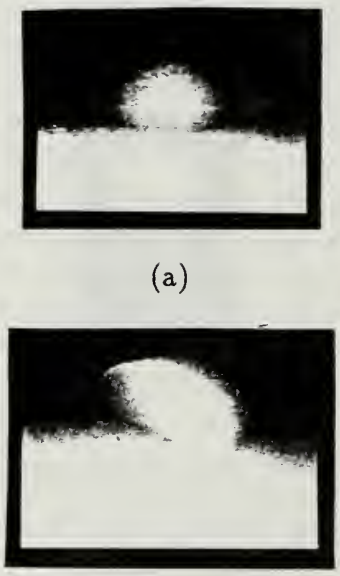

(a)

(b)

Figure 3.4: SAMPLE VISUAL PERSPECTIVE IMAGES OF SUBMERGED TARGETS a) Sphere with 100 cm radius, b) Cylinder (45° orientation, 100 cm horizontal offset) with 100 cm radius and 100 cm length. (Height of target center above bottom=0 cm (half-submerged), horizontal distance from sonar=450 cm, sonar height =200 cm, distance of image plane from sonar=100 cm.)

is visible in this case and it merges with the background at longer ranges. These figures serve as pictorial references of the scenarios presented to the sonar for subsequent acoustic imaging.

The 3–d coordinates of the imaged target voxels are also stored in a sequential formatted file "PERSVIS3.XYZ". (The run–file for this program is "PERSVIS3.EXE".)

At this stage the basic target data in the form of the visible target voxel coordinates is available. This is required for computing the target echo contribution to the acoustic image. The next chapter discusses the formation of the acoustic images by the sonar model.

Chapter 4

ACOUSTIC IMAGING PROGRAM

4.1 INTRODUCTION

The acoustic imaging program is the crux of the simulation model. The program takes the visible target voxels as primary input for developing the acoustic image. The sonar's system parameters and the sea–bottom backscatter characteristics are built into the model for a fairly comprehensive simulation. The sonar is assumed to uniformly insonify an azimuthal sector which is then scanned by a beam of a certain beamwidth. The return signal is assumed to be processed in a receiver that compensates for the spreading and absorption losses occurring in the water. The basic image format is the standard B–scan which paints range and bearing as rectangular coordinates. The B–scan format adopted in this model consists of 101 bearing cells plotted horizontally and 400 range cells plotted vertically. The acoustic image has range increasing from 0 to 399 and the bearings vary from -50 to $+50$ from left to right. (The acoustic images shown in this report are only a part of the B–scan images in the region of interest around the objects.) The cell sizes are defined in terms of the bearing and range resolution of the sonar. The image intensity is stored as an 8-bit word after the necessary normalization.

The program basically provides three acoustic images for purposes of further processing: B–scan image of target alone (BSCAN3.IMG), composite B–scan image of target with bottom backscatter (BSCAN3SH.IMG), and a

modified B–scan image to demonstrate the silhouette (SIL.IMG). The details of the program are discussed below. (The run–file of this program is "IMAG1.EXE".)

4.2 TARGET IMAGING

As discussed in the previous chapter the file "PERSVIS3.XYZ" stores the coordinates of the visible target voxels from the viewpoint of the camera (which is the sonar location). These visible voxels are those that happen to be perspectively imaged onto the image plane. Depending on the target imaging geometry and the visual resolution, the number of voxel coordinates stored is usually a small percentage of the 3–d surface points that were originally computed. (A value of 1% is a representative figure.) This implies extensive data reduction in the process of visual image formation and conveniently saves on computation time in the echo formation model. It should be borne in mind that each target voxel intrinsically represents a surface patch on the contiguous surface of the target, which in the first instance, had necessarily to be quantized for representation in a digital computer. This, coupled with the possibility of more than one adjacent target voxels being imaged on the same visual pixel, makes it essential to consider the size of the surface patch represented by an "imaged voxel" in the accurate computation of the echo intensity.

The area represented by this surface patch has dimensions that are inversely proportional to the distance of the image plane from the origin (F_i) and proportional to the horizontal distance of the voxel from the origin (X_t). The signal level contributed by this surface is made proportional to its area. It is apparent that surface patches at the same horizontal distance would have the same dimensions and those at longer ranges would have larger dimensions. The dimensions of the surface patch are X_t/F_i.

The selection of F_i should be so made such that the surface patch dimensions over the visible extent of the target are smaller than at least half the acoustic wavelength. Since the model considers the surface patches to be point reflectors for the purpose of signal contribution, the separation between adjacent patches should be very small (relative to the wavelength) for them to accurately represent an acoustically contiguous surface. For example, consider imaging a sphere of radius 100 cm at a horizontal distance of

500 cm from a sonar operating at a wavelength of 8 cm. The sphere's visible surface would lie between the horizontal range interval of 400 cm to 500 cm. If we choose F_i to be 50 cm, then the surface patch dimensions would lie between 8 cm and 10 cm over the target's visible region. This violates our constraint as it exceeds 4 cm (half wavelength). A choice of F_i as 125 cm or more would meet our requirement. Conversely, the wavelength can be chosen to be sufficiently large to satisfy this condition. (This constraint on F_i is imposed in addition to an earlier restriction discussed in the previous chapter that guarantees the opacity of the visual image.) The constraint on F_i for accurate acoustic imaging may be written as

$$\frac{X_t(\max)}{F_i} < \frac{\lambda}{2}, \tag{4.1}$$

where $X_t(\max)$ is the horizontal distance of the farthest imaged voxel and λ is the acoustic wavelength corresponding to the cw pulse carrier frequency.

The above constraint on F_i can now be combined with the one expressed in Eq. 3.4 as

$$\frac{2X_t(\max)}{\lambda} < F_i < \frac{X_t(\min)}{2}. \tag{4.2}$$

Once this is done, the program proceeds to calculate the complex signal returns (amplitude and phase) from each voxel contained in the file "PERSVIS3.XYZ". The program can currently process only 5,000 voxels due to memory limitations. (This number can be raised by a better memory budgeting but has been seen to be more than adequate for the scenarios of interest.) The program performs a running coherent sum of individual signals contributed by the target voxels within the range–bearing cell under consideration. Referring to Figure 4.1, for example, the signal contributions of the target voxels are calculated as shown below:

$$S_1 = A_1 \exp(-2jkR_1) \tag{4.3}$$
$$S_2 = A_2 \exp(-2jkR_2) \tag{4.4}$$

where

- S_1, S_2 = signals contributed by the two voxels,
- A_1, A_2 = surface patch areas represented by the visual pixels,

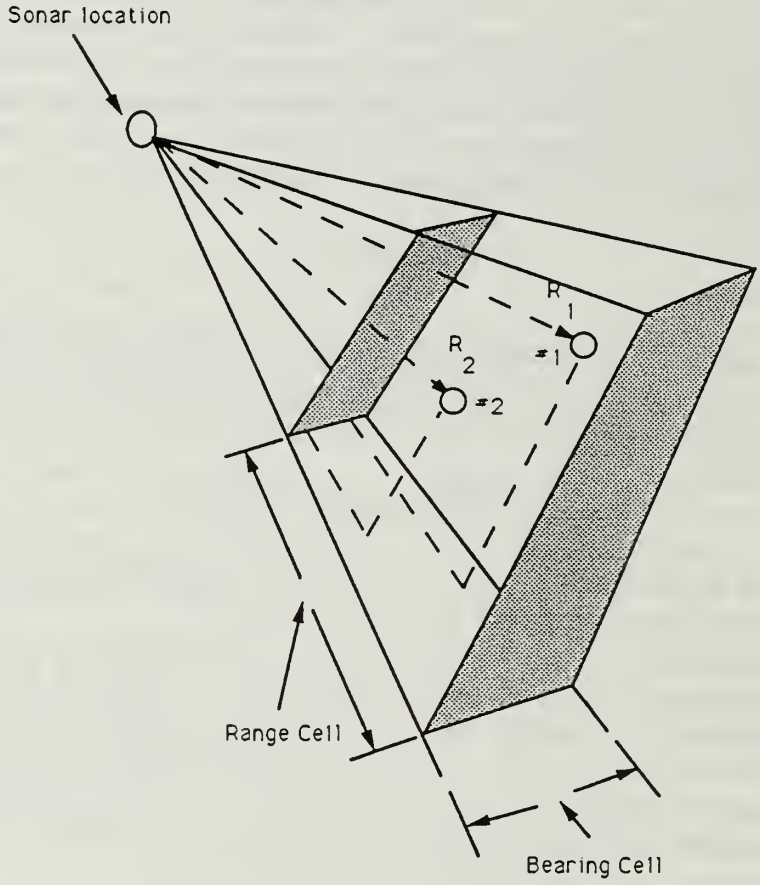

Figure 4.1: SIGNAL CONTRIBUTIONS OF TARGET VOXELS

a) Sphere (as in Fig. 3.3a)

b) Cylinder (as in Fig. 3.3b)

c) Sphere (as in Fig. 3.4a)

d) Cylinder (as in Fig. 3.4b)

Figure 4.2: SAMPLE B–SCAN TARGET ECHO IMAGES. (Range resolution = 20 cm, bearing resolution = 2.5°, wavelength = 8 cm.)

- $k = 2\pi/\lambda$, and
- R_1, R_2 = radial distance of the voxels from the sonar.

After all voxels are accounted for, the program generates its first B–scan acoustic image "BSCAN3.IMG". The acoustic image is formed by computing the (scalar) magnitude of the summed signals for each range–bearing cell. For ease of display the image is normalized to a maximum level of 255. Figures 4.2a and b are the sample B–scan acoustic images for the target scenarios shown in Figures 3.3a and b, respectively. (The horizontal axis is bearing and the vertical axis is range.) Figures 4.2c and d are the corresponding B–scan acoustic images for the scenarios shown in Figs. 3.4a and b, respectively. The images are formed from a single acoustic pulsed transmission with the parameters mentioned in the caption of Fig. 4.2 and demonstrate the specular target echoes that typically characterize acoustic images.

4.3 BOTTOM BACKSCATTER

The bottom backscatter calculation is done on the basis of the bottom surface area exposed to the acoustic beam in each range–bearing cell. The area of the sea bottom on a range–bearing cell basis in the absence of the target is first calculated. Thus, cells at the same radial range from the sonar have the same area. The initial cells prior to the sea–bottom do not contribute any backscatter in our simulation. (It should be possible to include volume backscatter at this point. We have ignored it for the present, however, as it is presumed to be too weak relative to the bottom backscatter.) A record is also kept of the grazing angle of each cell for subsequent calculation of the angle–dependent backscatter.

Next, we compute the range and bearing extent of the shadow of each of the visible target voxels on the sea–bottom. As explained earlier for the case of target imaging, the dimensions of the voxels are taken into account for these calculations. The area of the shadow regions is subtracted from the total bottom area on a range–bearing cell basis. The resultant area is the actual bottom area contributing to backscatter (Fig. 4.3). The backscatter is computed by multiplying these areas by the corresponding grazing–angle–dependent terms as per Lambert's law.

The raw backscatter so computed is further multiplied by a random number taken from either the uniform or Rayleigh distributions to simulate the selected statistics:

$$P_B = A_B \times \sin^2(\theta) \times \mathrm{RND} \tag{4.5}$$

where

- P_B is the backscatter power,
- A_B is the net bottom area exposed in a range–bearing cell,
- θ is the grazing angle of incidence to the above area, and
- RND is a number from a random distribution (else unity for non–random backscatter).

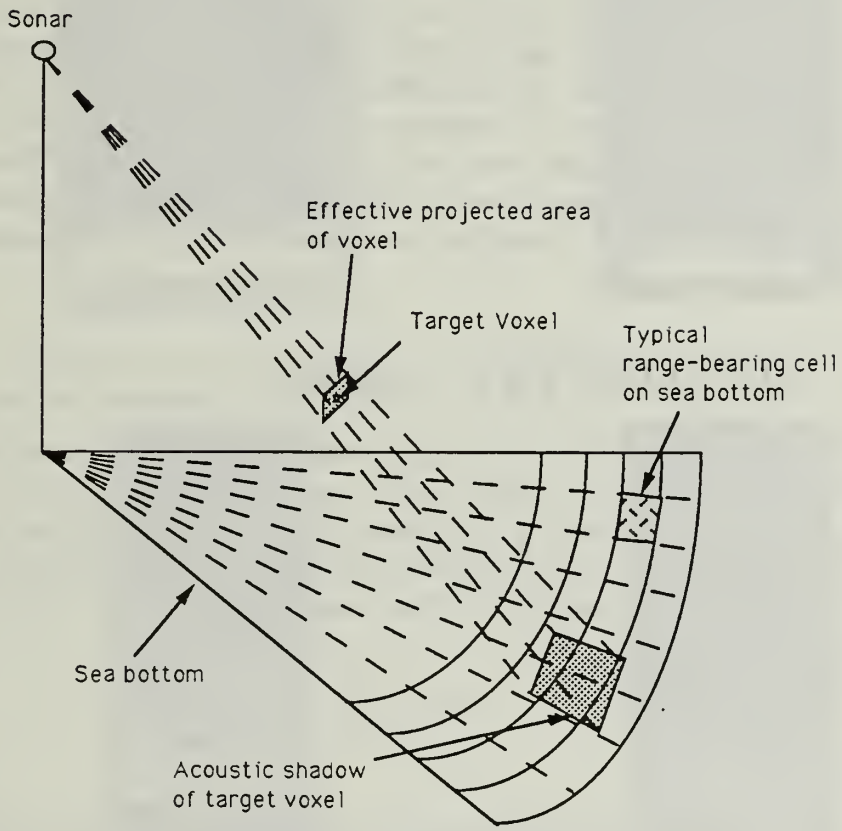

Figure 4.3: BOTTOM BACKSCATTER AREA SHOWING ACOUSTIC SHADOW STRADDLING RANGE-BEARING CELL BOUNDARIES.

4.4 COMPOSITE ACOUSTIC IMAGE

The composite acoustic image of the 3–d target against the sea–bottom is generated by the incoherent summation of the target echoes and the backscatter returns. The signal intensity is normalized to a maximum level of 100 and stored as a B–scan image in the file "BSCAN3SH.IMG". Sample composite acoustic images are shown in Figure 4.4. (These images correspond to the images in Fig. 4.2.) Figures 4.4a and b are for a constant Lambertian backscatter and Figs. 4.4c and d are for the random backscatter condition. These images demonstrate the formation of the acoustic shadow on the sea bottom. (Depending upon the relative strength of the target echo and the local backscatter, the target echo may or may not be visible.) These composite acoustic B–scan images are the simulated images of the scenario that would be generated by an imaging sonar with the chosen parameters and backscatter type.

4.5 SILHOUETTE IMAGE

The "BSCAN3SH.IMG" file shows the acoustic shadow of the target in an exaggerated manner. This shadow can be used to obtain the silhouette of the object by appropriate warping of the range axis. The approach we have used is basically a conversion of the "plan–type image" into a perspective image of the sea–bottom as viewed from the sonar location. The transformation applied to the range–axis is

$$R_M = \frac{H}{R_G} \tag{4.6}$$

where

- R_M is the modified range scale for converting from B–scan to silhouette image,
- H is the sonar height,
- $R_G = \sqrt{R_s^2 - H^2}$ is the ground range, and
- R_s = slant range.

a) Sphere (as in Fig. 4.2a)
Constant Lambertian backscatter

b) Cylinder (as in Fig. 4.2b)
Constant Lambertian backscatter

c) Sphere (as in Fig. 4.2c)
Rayleigh backscatter

d) Cylinder (as in Fig. 4.2d)
Uniform backscatter

Figure 4.4: SAMPLE COMPOSITE B-SCAN IMAGES

a.) Sphere (from Fig. 4.4a).

b) Cylinder (from Fig. 4.4b).

Figure 4.5: SAMPLE SILHOUETTE IMAGES

The effect of this transformation is to compress the range axis in a non–linear manner. The image intensity stored at each modified range cell is the minimum intensity in the range interval represented by the compressed cell. This is done to highlight the shadow regions.

The new image is recorded in a pseudo–B–scan format and shows the silhouette in a geometrically accurate form. It is to be noted that the transformation of Eq. 4.6 is only to be used as an aid for target identification from its shadow alone and not from its echo. The range warping effect on the echo region should not be directly used for any interpretative work.

The silhouette–image as obtained above is stored in the file "SIL.IMG". Sample silhouette images are shown in Figure 4.5. These are generated from the composite B–scan images of Fig. 4.4a and b. The nonlinear range transformation compresses the far–field and expands the near–field. Consequently, the shadows become shortened and the target echoes, which are near, become stretched. The resulting shadows represent the silhouettes of the sphere and cylinder shown in Fig. 3.3. These images demonstrate the effectiveness of the range scale transformation applied to the B–scan images for obtaining the

silhouette images. The silhouette images compare favorably with the visual perspective images of the respective objects as shown in Fig. 3.3.

The computer model at this stage represents the simulation of acoustic images from a sector–scanning sonar in the specified scenario. A first step towards object classification has also been taken with the extraction of the silhouette image from the shadow extent of the target in its acoustic image. In the following chapter we present the next step towards classification, the 3–d reconstruction of the confining volume of the target's visible surface. In this approach we utilize both the shadow and range extents of the target.

Chapter 5

TOWARDS 3–D RECONSTRUCTION

5.1 INTRODUCTION

The previous chapter has demonstrated the generation of acoustic images of 3–d objects against the sea–bottom in the conventional B–scan format. It is well–known that interpretation of these images requires skilled operators who have had extensive training and experience in the operation and use of such imaging sonars. As the demand and applications of these sonars increase, it is obvious that the trained human element is likely to be in short supply. Some applications may, in fact, require a machine to sift through the data and draw its own conclusions from the acoustic images. The above statements point to the need for a more useful image presentation that makes it easier for an unskilled operator to interpret the acoustic images by making use of some clues that a trained operator would utilize in the classification process. This chapter discusses the first attempt towards generation of 3–d images of the acoustically visible surface for targets whose echo and shadow regions do not overlap.

5.2 SEGMENTATION

A primary function of an image–processing system is to segment a raw image from the sensor into appropriate regions. In our case we are interested in

segmenting the acoustic image into three regions: echo, shadow and bottom–backscatter. The composite acoustic image file "BSCAN3SH.IMG" is processed by a dual threshold derived from the image itself in the following manner:

1. The average signal intensity at each range is computed.
2. The echo region is extracted if the image intensity exceeds the range–average by more than 20%.
3. Those pixels that lie below this threshold are again compared with a threshold that is 70% of the range average to distinguish between the backscatter and the shadow regions.
4. The echo region is labeled as region "2", the backscatter as region "1", and the shadow as region "0".

The segmentation result is stored in tabular form in a sequential formatted file "SEGEXT". This file stores the range limits of the target echo and shadow regions at each bearing. A segmented B–scan image is also displayed on the monitor for checking the quality of the segmentation process. The run–file for the segmentation program is "SEG2.EXE".

The segmentation has presently been attempted against Lambertian backscatter. We have for the present avoided getting into the details of image segmentation in random backscatter since it detracts from the immediate task of 3–d reconstruction. (The 3–d reconstruction presupposes a good segmentation of the acoustic image which, in principle, can be done for the other cases of backscatter.)

5.3 CONFINING VOLUME

The segmented image provides volumetric information about the visible region of the target. This information resides directly in the range extent of the target echo and indirectly in the range extent of the shadow. The shadow extent in a particular bearing is easily translated into vertical angular extent for targets with distinct echo and shadow regions as per the following (Fig. 5.1):

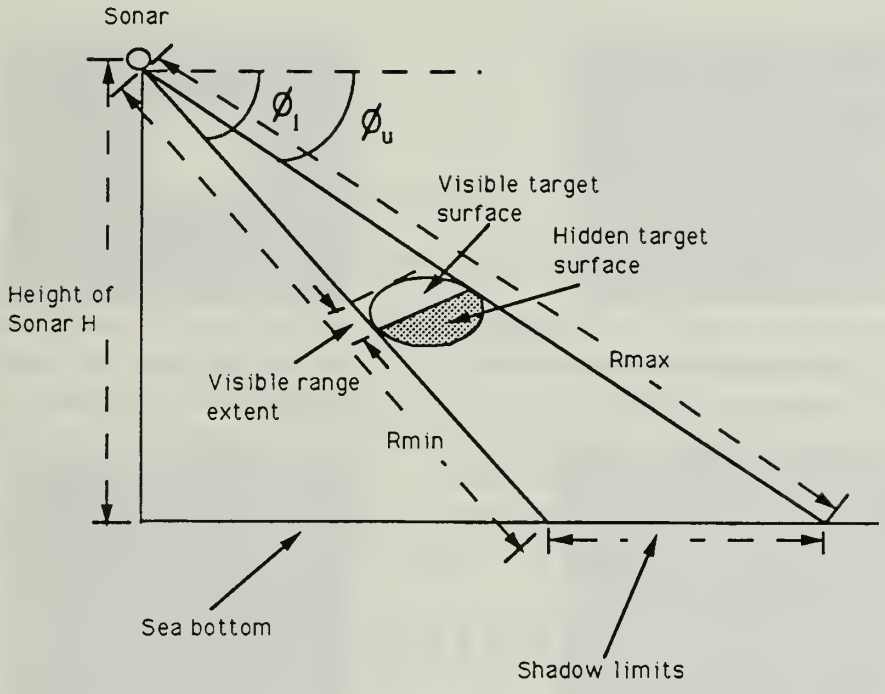

Rmin, Rmax : sonar range at shadow limits

Figure 5.1: VERTICAL ANGULAR EXTENT FROM SHADOW LIMITS

$$\phi_u = \sin^{-1}\left(\frac{H}{R_{\max}}\right) \tag{5.1}$$

$$\phi_l = \sin^{-1}\left(\frac{H}{R_{\min}}\right). \tag{5.2}$$

where

- ϕ_u = upper angular limit,
- ϕ_l = lower angular limit,
- $R_{\max}$ = far range of the shadow extent, and
- $R_{\min}$ = near range of the shadow extent.

The angles ϕ_l and ϕ_u are referenced below the horizon. The visible surface of the target can be safely assumed to be confined within the range and angular extents as computed above. This confining volume can be regarded as a stack (in bearing) of vertical circular sectors lying within the minimum and maximum range radii of the echo.

The 3-d coordinates of the above slices are computed by the run-file "RAW1-3D.EXE" and stored in a sequential formatted file "RAW-3D".

5.4 3–D WIRE–FRAME IMAGE

The information derived above is suitable for presentation in a more conventional visual form as a perspective image. This represents a fundamental break from the direct acoustic image obtained from the sonar. The additional range information available to us can be used to advantage in the generation of the acoustically-derived perspective image. We have written a program that can artificially view the confining volume from different vantage locations around the target to heighten the depth perspective. The run-file that generates the wire-frame perspective image is "RAWIRE1.EXE" and the image is stored in a sequential binary file "RAWIRE.IMG". This image is generated in a 250 x 250 pixel range-shaded format like the visual images generated earlier. Sample wire-frame images are shown in Figure 5.2. Figure 5.2a shows the visual perspective image of a sphere. Figures 5.2b–

a) Sphere (Fig. 3.3a)
Visual perspective image

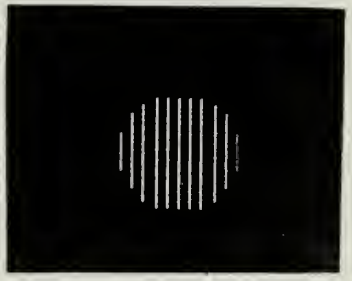

b) Wire–frame image
Viewing angle: 0°

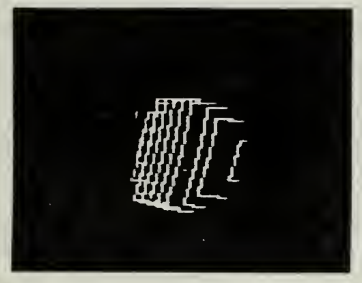

c) Wire–frame image
Viewing angle: 20°

d) Wire–frame image
Viewing angle: 40°

Figure 5.2: SAMPLE WIRE–FRAME IMAGES (Swivel radius for viewing wire–frame = 550 cm).

d show different views of the wire–frame image of this sphere constructed from the echo and shadow range extents in its composite acoustic image of Figure 4.4a. A hypothetical camera is swiveled around the wire–frame image in a circular arc of a selectable radius. The angle on this arc relative to the sonar's broadside direction specifies the camera's vantage location for viewing the wire–frame image.

Chapter 6

CONCLUSIONS

6.1 INTRODUCTION

This report has discussed the implementation of a computer model of a sector–scanning sonar for imaging of objects against the sea–floor. The entire simulation exercise is carried out on an IBM PC–AT–compatible computer. Based upon the acoustic images simulated, wire–frame perspective images of the confining volume of the target's visible surface have been generated. The images are recorded in binary files in a format suitable for viewing and hardcopying using the "PCVISIONplus" system.

6.2 CAPABILITIES OF THE MODEL

The computer model has a number of interesting features as listed below:

- It simulates spherical and cylindrical targets of different dimensions and at various orientations relative to the sonar and the sea–bottom (including partially submerged targets).
- The operator can specify the beamwidth, range resolution and wavelength of the sonar.
- The bottom backscatter statistics are selectable between uniform, Rayleigh, and constant (i.e., Lambertian alone).
- It generates visual perspective images.

- It intrinsically models specular reflections and acoustic shadows.
- It generates silhouette images.
- The model also generates 3–d wire–frame images of the visible confining volume (of suspended targets) that are viewable from various vantage locations.

6.3 POSSIBLE ENHANCEMENTS

The computer model developed thus far is a framework under which further enhancements can be incorporated in a straight–forward manner. Some of the possibilities are:

1. a more extensive library of targets,
2. inclusion of volume backscatter,
3. a larger variety of bottom backscatter statistics, and
4. segmentation in the presence of specular backscatter.

The confining volume image is proposed to be refined into a more exact shape of the visible surface by inclusion of other clues like echo intensity. The image reconstruction attempted in this report is for targets whose echo and shadow regions are non–overlapping. Work is presently underway to study the problem of reconstructing targets whose echo and shadow regions overlap, as is the case for targets lying on the sea–bed.

6.4 CONCLUSION

The computer model, in addition to being a simulator of the acoustic imaging process, is also a powerful tool for carrying out developmental studies for 3–d reconstruction and classification of objects by means of a sector scanning sonar.

6.5 ACKNOWLEDGEMENTS

This work was done while Rajendar Bahl held a National Research Council – Naval Postgraduate School Research Associateship on leave from the Indian Institute of Technology, New Delhi.

References

[1] M.L. Somers and A.R. Stubbs, "Sidescan sonar," *IEE Proc.*, Vol. 131, Part F, No.3, pp. 243–256, June 1984

[2] R.B. Mitson, "Review of high–speed sector–scanning sonar and its application to fisheries research," *IEE Proc.*, Vol 131, Part F, No. 3, pp. 257–269, June 1984

[3] J.L. Sutton, "Underwater Acoustic Imaging," *Proc. of IEEE*, Vol. 67, No. 4, pp. 554–566, April 1979

[4] P.T. Gough, "A synthetic aperture sonar system capable of operating at high speed and in turbulent media," *IEEE J. Oceanic Eng.*, Vol. OE–11, No. 2, pp. 333–339, April 1986

[5] P.T. Gough, A. de Roos and M.J. Cusdin, "Continuous transmission FM sonar with one octave bandwidth and no blind time," *IEE Proc.*, Vol. 131, Part F, No. 3, pp. 270–274, June 1984

[6] T.L. Henderson, "Wideband monopulse sonar: Processor performance in the remote profiling application," IEEE J. Oceanic Eng., Vol. OE–12, pp. 182–197, Jan. 1987

[7] R. Bahl and O. George, "Computer simulation of a high resolution sonar," Technical Report, CARE, IIT Delhi, New Delhi, Dec. 1988

[8] B.D. Steinberg, "Aperture Fundamentals," in *Principles of Aperture and Array System Design*, Chapter 1, John Wiley & Sons, Inc., 1976

[9] R.J. Urick, *Principles of Underwater Sound*, McGraw–Hill, New York, 1975

[10] N.P. Choitros, H. Boehme, L.D. Rolleigh, S.P. Pitt, A.L. Garcia, T.G. Goldsberry, and R.A. Lamb, "Acoustic backscattering at low grazing angles from the ocean bottom. Part I. Bottom backscattering strength," *J. Acoust. Soc. Am.*, Vol. 77, No. 3, pp. 962–974, Mar. 1985

[11] H. Boehme, N.P. Choitros, T.G. Goldsberry, S.P. Pitt, R.A. Lamb, A.L. Garcia, and R.A. Altenburg, "Acoustic backscattering at low grazing

angles from the ocean bottom. Part II. Statistical characteristics of bottom backscatter at a shallow water site," *J. Acoust. Soc. Am.*, Vol. 77, No. 3, pp. 975–982, Mar. 1985

[12] A.C. Bovik and D.C. Munson, Jr., "Boundary detection in speckle," *Proc. of Int'l. Conf. on Acoust. Speech & Signal Process.*, Tampa, Florida, pp. 893–896, IEEE Press, 1985

Appendix A

OPERATING GUIDE

A.1 HARDWARE REQUIRED

The following hardware is required for the operation of the computer model:

- An IBM PC–AT (or compatible) with 640KB RAM, hard disk, 360 KB floppy drive
- "PCVISIONplus" system (from Imaging Technology Inc.) installed on the PC including a B/W video monitor
- Hardcopy unit TEKTRONIX Model HC01 (optional)

A.2 OPERATING STEPS

The operating steps to be followed are:

1. Execute file "CIRCLE.EXE"
2. Execute either file "SPHERE3.EXE" or "CYL.EXE"
3. Execute file "PERSVIS3.EXE"
4. Execute file "IMAG1.EXE"
5. Execute file "SEG2.EXE"

6. Execute file "RAW1-3D.EXE"
7. Execute file "RAWIRE1.EXE"

The following images are generated for viewing:

1. "PERSVIS3.IMG" at step (3)
2. "BSCAN3.IMG", BSCAN3SH.IMG", and "SIL.IMG" at step (4)
3. "RAWIRE1.IMG" at step (7)

The executable program files are available from:

Professor John P. Powers
Dept. of Electrical and Computer Engineering
Naval Postgraduate School
Monterey, CA 93943

DISTRIBUTION LIST

		No. Copies
1.	Defense Technical Information Center Cameron Station Alexandria, VA 22304–6145	2
2.	Library, Code 0142 Naval Postgraduate School Monterey, CA 93943–5002	2
3.	Department Chairman, Code EC Naval Postgraduate School Monterey, CA 93943–5004	1
4.	Director of Research Administration, Code 012 Naval Postgraduate School Monterey, CA 93943–5000	1
5.	Professor John Powers, Code EC/Po Naval Postgraduate School Monterey, CA 93943-5002	10
6.	National Research Council Attn: Research Associateship Programs 2101 Constitution Ave. Washington, DC 20418	1
7.	Head Center for Applied Research in Electronics Indian Institute of Technology New Delhi, 110016 INDIA	1

8. Dr. Rajendar Bahl — 10
Center for Applied Research in Electronics
Indian Institute of Technology
New Delhi, 110016
INDIA

9. Chairman — 1
Working Group S-UWES
Department of Electronics
Lok Nayak Bhawan
New Delhi, 110003
INDIA

10. Dr. V.P. Kodali — 1
Adviser
Electronics Commission
Lok Nayak Bhawan
New Delhi, 110003
INDIA

11. Professor A.K. Jain — 1
Department of Computer Science
Michigan State University
A-726 Wells Hall
East Lansing, Michigan 48824-1027

12. Dr. John C. Hyland — 1
Code 2220
Naval Coastal Systems Center
Panama City, FL 32407-5000

13. Dr. R.H. Evans, Head — 1
Undersea Technology, Code 7021
Naval Undersea Warfare Engineering Station
Keyport, WA 98345

14. Professor A. Rosenfeld, Director 1
Center for Automation Research
University of Maryland
College Park, MD 20742